Interrogation of interferometric sensors with a tilted fiber Bragg grating

César Jáuregui, José Miguel López-Higuera, Antonio Quintela

Grupo de Ingeniería Fotónica –Universidad de Cantabria
E.T.S.I.I. y Telecomunicación – Dpto. TEISA
Avda. Los Castros s/n – c.p. 39005 Santander, Spain
Tel: ++ 34-942-200877 ext. 16; Fax: ++ 34-942-200877
jauregui@teisa.unican.es

Abstract: This paper describes the interrogation of interferometer-based transducers with a technique that involves the use of a tilted fiber Bragg grating. The interrogation process will be analyzed both from the conceptual and experimental points of view. Simultaneous interrogation of multiplexed interferometric transducers is successfully checked using this technique.

OCIS codes: (060.2370) Fiber optics sensors; (120.3180) Interferometry.

References and Links

1. J.M. López-Higuera, editor, *Handbook of Optical Fiber Sensing Technology* (John Wiley Ed., 2002).
2. A.D. Kersey, M.A. Davis, H.J. Patrick, M. LeBlanc, K. P. Koo, C.G. Askins. M.A. Putnam and E.J. Frieble, "Fibre grating sensors," J. Lightwave Technol. **15**, 1442-1463 (1997).
3. J.L. Santos, A.P. Leite and D.A. Jackson, "Optical fiber sensing with a low-finesse Fabry-Pérot cavity," Applied Optics **31**, 7361-7366 (1992).
4. Y. Botsev, N. Gorbatov, M. Tur, U. Ben-Simon, I. Kressel, A.K. Green, G. Ghilai, S. Gali, "Fiber Bragg grating sensing in smart composite patch repairs for aging aircraft," J.M. López-Higuera and B. Culshaw, eds., *Proceedings of the EWOFS'04*, Proc. SPIE **5502**, 100-103 (2004).
5. P. Nash, "Review of interferometric optical fibre hydrophone Technology," *Proceedings of IEE* **143**, 204-209 (1996).
6. C. Jáuregui, A. Quintela, J.M. López-Higuera, "Interrogation Unit for Fiber Bragg Grating Sensors that Uses a Slanted Fiber Grating," Opt. Lett. **29**, 676-678 (2004).
7. J. Kusuma, "Parametric Frequency Estimation: ESPRIT and MUSIC" (2002).
8. C. Jáuregui, A. Quintela, F.J. Madruga, A. Cobo, J.M. López-Higuera, "Fiber Bragg Grating Interrogation Scheme Based on the Radiated Near-Field of a Tilted Fiber Grating," *Proceedings of the OFS'16*, K. Hotate, ed., (Nara, Japan, 2003), 702-705.
9. S. Haykin, *Adaptative filter theory* (Ed. Prentice Hall, 2nd Edition, 1991).

1. Introduction

Photonic sensor systems are becoming increasingly popular nowadays. This is because there are several fields (aeronautics, civil engineering, nuclear industry, etc) that can greatly benefit from their characteristics: low weight and size, immunity against electromagnetic interference, multiplexing capabilities, etc. However, in spite of these advantages, the field has not experienced a commercial boom yet. This is mainly because of the natural reluctance of the market with respect to new technologies and to the higher unitary costs of this kind of transducers when compared to traditional ones. Both of these problems can be overcome with time and mass-production. Nevertheless, there is still another problem which demands a big research effort to be solved: the interrogation of photonic transducers. Lot of work has been done in this topic in the last years [1], but very few of the interrogation techniques that came up as a result of that research can be used in a real-world environment. And those which can work in real applications are usually very expensive and have been specifically designed to interrogate just one kind of transducers. This fact constitutes an important brake for the

#5299 - $15.00 US Received 15 September 2004; revised 3 November 2004; accepted 4 November 2004

commercial success of photonic sensing. Thus, the field will benefit a lot from low-cost multi-transducer interrogation units.

Among the different technologies included in the photonic sensing field there are two of special relevance: Fiber Bragg Gratings (FBG) [2] and interferometers [3]. These are the most widely used devices in the field due, mainly, to their versatility (first case) and high sensitivity (second case). Thus, FBGs have been and still are extensively used in civil engineering applications and in the aerospace industry [4], and interferometers are gaining an increasing popularity as hydrophones [5]. So, taking these facts into account, and reckoning the demand for multi-transducer interrogation units, the authors have very recently presented a technique that can be used for recovering the measured information from both FBGs and interferometers. At first this technique was developed for the interrogation of FBGs [6]. This paper presents the adaptation of that technique for the interrogation of reflective interferometer-based transducers (Fabry-Pérot cavities or Michelson interferometers) and, therefore, the demonstration of this technique as being multi-transducer.

The proposed interrogation technique involves the use of a tilted and chirped fiber Bragg grating (TCFBG) placed in front of a photodetector linear array. In these circumstances the TCFBG expels some light which is captured by the linear array in the form of images. By processing these images with an adaptative digital filter, a representation of the light's spectrum can be obtained. From this spectrum the information measured by the interferometric transducer can be recovered simply by using a period estimation algorithm. In this case it was a modified version of the MUSIC algorithm [7], which will be explained in detail in the paper. This algorithm represents an alternative to the FFT-based frequency estimation methods and performs slightly better.

The present paper reports the different steps required to make the initial FBG interrogation technique able to extract information from interferometer-based transducers. Since those sensors are very different in nature to FBG, this adaptation requires profound changes in the processing algorithms of the interrogation system. Moreover, in this chapter a new cavity-length estimation algorithm has been developed and tested in the works reported here. This algorithm is based on the MUltiple SIgnal Classification algorithm (MUSIC), and will be explained in detail in the following lines. Besides, the system as a whole is tested in several experiments to obtain a preliminary idea of its potential performance when interrogating interferometers. In summary, this paper gives an overview of a new interrogation technique stressing the most important contributions that are the new algorithm and the experimental characterization. The paper is organized as follows: at first a conceptual explanation of the operating principle is carried out, later on several experimental results are presented and discussed and, finally, some conclusions are extracted.

2. Operating principle

This section starts with a brief revision of the basics of the proposed interrogation technique, although they have been presented elsewhere [8].

As has been outlined in the introduction, the system comprises a TCFBG placed in front of a photodetector linear array and separated from it a few millimeters. This has been schematically represented in Fig. 1. It is widely known that tilted gratings are able to extract some portion of the light that propagates through the fiber. This extraction takes place all along the length of the TCFBG and, thus, when using a linear array to detect this expelled light, an image will be seen. The TCFBG extracts light in the whereabouts of a central wavelength which is determined by the period of the grating and the tilt angle. This region can be as wide as 150nm or even more. The characteristics of the radiated light are highly wavelength-dependent, which ultimately means that the radiation images recorded by the linear array will change with wavelength. Moreover, each radiation image corresponding to a particular wavelength is unique. This point is truly important in this system since it allows for the determination of the wavelength of the radiated light by analyzing the characteristics of the image. Namely the characteristics under study should be shape and position. The first one is the most important and its analysis is performed by a pattern recognition algorithm

#5299 - $15.00 US Received 15 September 2004; revised 3 November 2004; accepted 4 November 2004

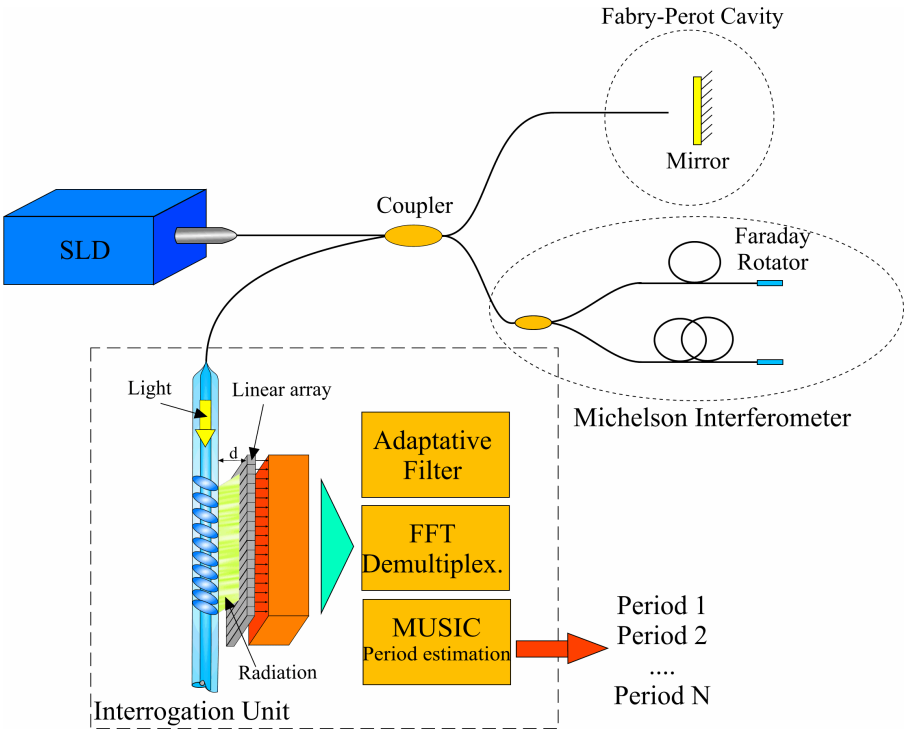

Fig. 1. Block diagram of the proposed interrogation technique for reflective interferometer-based transducers.

implemented with a modified version of the Kalman adaptative digital filter [9]. The second characteristic comes from the fact that the output angle of the radiated light changes with wavelength. This, at the end, means that the image recorded by the array will shift. This shift makes things easier for the pattern recognition algorithm. The latter also explains the reason why this shift has been promoted by heavily chirping the tilted grating.

The above explained procedure is quite simple when the radiated light is monochromatic. However, it becomes rather difficult for broadband light. This is because, as explained before, the radiation images are very wide (covering the whole length of the TCFBG). Therefore, the images corresponding to the "different wavelengths" of the broadband light will overlap creating, thus, a more complex image. This fact represents a difficult task since the problem now is not only trying to identify a pattern from a set of them contained in a database, but choosing the best combination of them to obtain a composite image as similar as possible to the recorded one. This task, which is the actual heart of the interrogation system, is carried out by the adaptative digital filter shown as a block in Fig. 1. After this processing an inaccurate representation of the light's spectrum is obtained. Although this spectrum is not the real one, it preserves some characteristics that make it useful for sensing. For example, when dealing with narrowband lights, the wavelengths of the peaks are very well determined although their amplitudes are inexact. This allows for the interrogation of FBGs. On the other hand, when interrogating interferometers, which is the main topic of this paper, the spectrum recovered after the digital filtering is somewhat distorted as shown in Fig. 2. There, the spectrum of a 193μm long low-finesse Fabry-Perot cavity (built placing the tip of a monomode standard optical fiber in front of a mirror) is shown. In this figure the same spectrum has been recovered by an optical spectrum analyzer (Fig. 2(a)) and by the interrogation technique proposed in this paper (Fig. 2(b)). In the latter case the spectrum shown in Fig. 2(b) is the one obtained after the adaptative filter stage of Fig.1. By comparison of the two graphs shown in Fig. 2, the amplitude distortion becomes evident. Despite this distortion, the interferometer

#5299 - $15.00 US Received 15 September 2004; revised 3 November 2004; accepted 4 November 2004

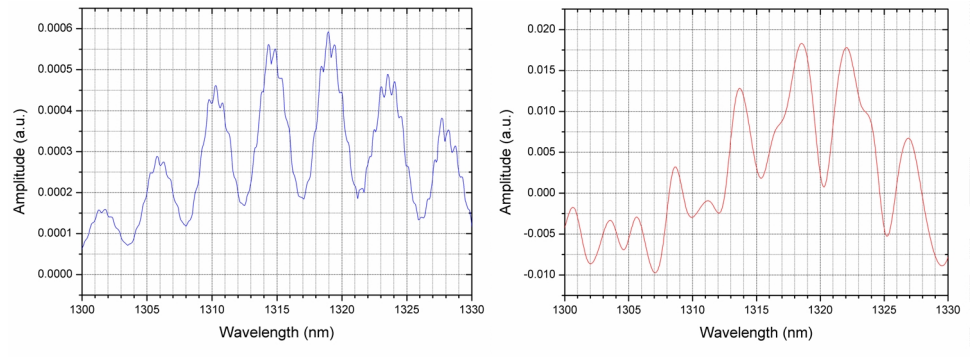

a) b)

Fig. 2. Spectra of a 193µm long low-finesse Fabry-Perot Cavity as recovered by: a) an Optical Spectrum Analyzer and b) the digital adaptative filter in the interrogation technique proposed in this paper.

path imbalance can still be recovered, provided appropriate algorithms are employed. Since the measured information is contained in the optical path imbalance, this technique allows for the interrogation of interferometer-based transducers.

After the digital filter, and in case there were several multiplexed transducers as shown in Fig. 1, a demultiplexing stage is required. This stage consists in a FFT-based bandpass filtering to separate the sinusoidal spectra of the different transducers. The need for this stage will become evident after the explanation of the optical path imbalance estimation algorithm.

The above mentioned distortion makes the recovery of the interferometer path imbalance (cavity length for Fabry-Perot Cavities) far from straightforward. Difficult to believe as it might be by having a look at Fig. 2, the information on the periodicity of the spectrum is preserved in the distorted image. However, it requires a sophisticate algorithm to recover it. This can be done using a period estimation algorithm, since the path imbalance can be recovered from the period of the interferometer's sinusoid spectrum. In this case the chosen one was a modified version of the MUSIC algorithm. This algorithm was originally designed for estimating the periods of sinusoidal signals in noise. The original version makes use of the fact that sinusoids of different frequencies are orthogonal. This implies that the autocorrelation function of a signal composed of N pure sinusoids in noise will include no cross-correlation terms. In other words, the autocorrelation matrix will have an eigenvector per sinusoid (those corresponding to the N greater eigenvalues) plus several more due to noise. Taking into account that the eigenvectors of a matrix are orthogonal, the product of those due to noise by those of the sinusoids should be zero. Thus knowing the algebraic expression of the eigenvectors, a frequency scan can be performed in that product. The frequencies at which the product goes to zero indicate the presence of a sinusoid in the signal. However, the sinusoids obtained from the spectra of the interferometers are not pure but chirped. The latter demands some modifications from the original MUSIC algorithm. These variations will be explained in the following.

The digitized spectrum of an interferometer (Fabry-Perot cavity, for example) takes the form of a chirped sinusoid, which can be expressed as:

$$x[n] = A_1 \cdot e^{j\frac{4\pi d}{n\lambda_s}} \tag{1}$$

where d is the length of the cavity (and therefore the parameter to recover), A_1 is the amplitude of the sinusoid (closely related with the visibility of the fringes), and λ_s is the sample wavelength. As has been previously said, the MUSIC algorithm departs from the

#5299 - $15.00 US Received 15 September 2004; revised 3 November 2004; accepted 4 November 2004

eigenvectors of the autocorrelation matrix of the signal. However, due to the particularities of the algorithm, it is required that the autocorrelation function be an exponential with a phase that exhibits a linear dependence with *k* (delay). Luckily, the autocorrelation function of (1) can be approximated by:

$$r_x[k] = |A_1|^2 A[k] \cdot e^{j\left(p_3 k^3 + p_2 k^2 + p_1 k\right)\frac{4\pi d}{\lambda_c^2}}; \quad \text{with } A[k] = \left|\text{sinc}\left(\frac{2\pi k d}{\beta}\right)\right| \tag{2}$$

where λ_c is the central wavelength of the wavelength range in which the approximation takes place. Besides, β is a constant related with the index of refraction of the cavity. Finally p_3, p_2, p_1 are other constants that help to fit the phase term. In the range that goes from 1300nm and 1325nm and for a sample wavelength of 0.1nm, the values of these constants are, respectively, p_1=1.0000057, p_2=7.6183e-5, p_3=4.472e-9. As can be seen, p_1 is several orders of magnitude higher than the others. This implies that, provided the values of the *k* parameter remain small (<10), they can be safely neglected. Moreover for those values $A[k] \approx 1$. With these approximations the autocorrelation function takes the desired exponential form without compromising the accuracy of the final result. Limiting the maximum value of *k* imposes a constraint just in the maximum number of multiplexed sinusoids that can be detected (8 for a maximum value of 10 for *k*).

The autocorrelation function is used to build the autocorrelation matrix:

$$R_x = \begin{pmatrix} r_x[0] & r_x[1] & \dots & r_x[M-1] \\ r_x[-1] & r_x[0] & \dots & r_x[M-2] \\ \dots & \dots & \dots & \dots \\ r_x[-(M-1)] & r_x[-(M-2)] & \dots & r_x[0] \end{pmatrix} \quad \text{with M} < 10 \tag{3}$$

This matrix has one eigenvector per complex sinusoid ($\hat{e}_i$) in the signal and several more ($\hat{u}_i$) due to the noise present in the recorded signal. The latter will also be those corresponding to the smallest eigenvalues. The eigenvectors corresponding to the sinusoid contributions take the form:

$$\hat{e}_i = \begin{pmatrix} r_x[0] \\ r_x[-1] \\ \dots \\ r_x[-(M-1)] \end{pmatrix} \tag{4}$$

As is widely known, the eigenvectors of a matrix are all orthogonal one to another. Therefore, for the case of only one complex sinusoid the product of the sinusoid eigenvector by one of the noise eigenvectors will be:

$$\hat{e}_1^{\,H} \cdot \hat{u}_i \approx \sum_{m=0}^{M-1} u_i[m] \cdot |A_1|^2 \cdot e^{-jp_1 \frac{4\pi d}{\lambda_c^2} m} = 0 \tag{5}$$

where the point between the vectors stands for scalar product, and the *H* subscript indicates Hermitian transpose. Besides, $u_i[m]$ represents the elements of the noise eigenvector. The last expression can be generalized in the following way:

#5299 - $15.00 US Received 15 September 2004; revised 3 November 2004; accepted 4 November 2004

$$\hat{e}(w')^H \cdot \hat{u}_i \approx \sum_{m=0}^{M-1} u_i[m] \cdot e^{-jw'm}; \quad \text{with } w' = \frac{4\pi d}{\lambda_c^2} p_1 \tag{6}$$

in which the term $|A_1|^2$ has been suppressed since it does not alter the position of the zeroes. Using Eq. (6) a frequency scan on *w*' can be performed and, from it, the frequencies of the sinusoids can be estimated. Then these frequencies *w'* can be translated into cavity lengths by means of the expression provided in Eq. (6). Moreover, since there are multiple noise eigenvectors, this procedure can be repeated for all of them (the scalar product of all those vectors with the sinusoid one will present a zero at the same frequency) and by averaging the resulting *w'*, the accuracy on the frequency estimation can be greatly increased.

However, there is still one more detail to deal with: the fact that the sinusoid spectrum of an interferometer is a real sinusoid formed by the addition of two complex sinusoids of opposite frequency. For the above procedure to be applicable to this case it is mandatory that the autocorrelation function has no cross-correlation terms between the two complex sinusoids. This is not true for the case of chirped sinusoids and leads to the necessity of overlooking the cross-correlation terms even though they exist. This approximation has proved to cause an error that is always below the 6%. Nevertheless, it imposes a very strict limitation: the approximation remains accurate as long as the signal comprises no more than two complex sinusoids (if this requirement is not fulfilled, the errors will grow very rapidly since the cross-correlation terms will be of significant value). So, if the signal is formed by more than one sinusoid a demultiplexing algorithm is required prior to the execution of this modified version of MUSIC, just as sketched in Fig. 1.

In spite of this adaptation that turns the estimated cavity length into approximate, it has been seen that it performs slightly better than the FFT.

3. Experimental results

A setup similar to that shown in Fig. 1 was built for testing the interrogation technique. The only difference is that the Michelson interferometer was replaced with another Low Finesse Fabry-Perot cavity (LFFPC) built by placing the tip of a fiber in front of a mirror. So the system had two multiplexed sensing LFFPCs, one of which had its mirror attached to a motorized translation stage. The broadband light source was a superluminiscent diode (SLD-1300 from Fiberon Inc.). The InGaAs photodetector linear array had 512 pixels and was 1.28cm long (Hamamatsu G8161-512S). The tilted and chirped FBG was placed 4.775mm away from the detector. It was written by the phase mask technique in standard telecommunication hydrogen-loaded fiber. In order to achieve the blaze of the grating periods the phase mask was tilted with respect to the fiber. As a result of the UV exposure the final grating was 1cm long, and presented a 34º tilt angle with a period raging from 0.525μm to 0.559μm. The maximum attenuation of its spectrum was around 50% at 1280nm. However, this grating was able to efficiently outcouple light in the wavelength range of 1250nm to 1350nm.

Several experiments were carried out to this system to test its performance. The first one was an accuracy and linearity experiment. In it only one LFFPC was used, and it consisted in progressively modifying the length of the cavity. The linear photodetector was configured to have a 5ms integration time and a 16bits A/D converter. The results of that experiment are shown in Fig. 3. There the length recovered by the interrogation technique (dotted line) is compared with the actual one (straight line). It can be seen that the agreement between these two graphs is pretty good. This implies that both the accuracy and linearity of the technique are good. The average length error was around 1.6μm in this case. This error keeps below the 1% threshold of the actual cavity length in the whole range shown in Fig. 3.

#5299 - $15.00 US Received 15 September 2004; revised 3 November 2004; accepted 4 November 2004

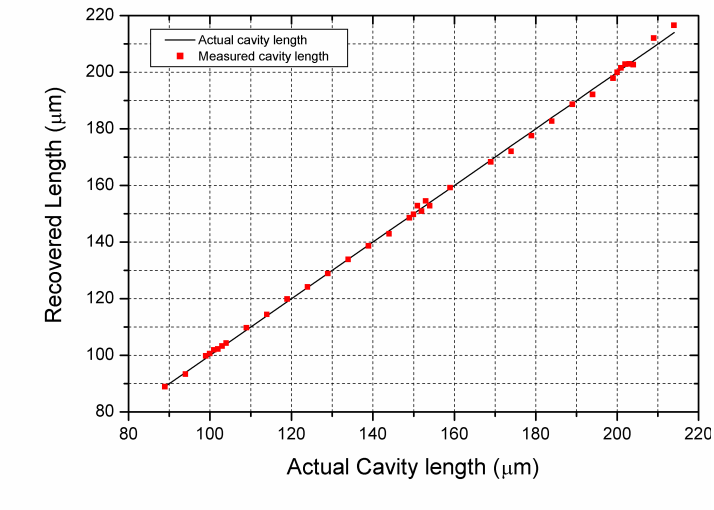

Fig. 3. Results of the cavity length sweep (dotted line) applied to a low-finesse Fabry-Perot cavity in comparison with the actual length (straight line). Experiment carried out with an integration time of 5ms and 16 bits of A/D conversion.

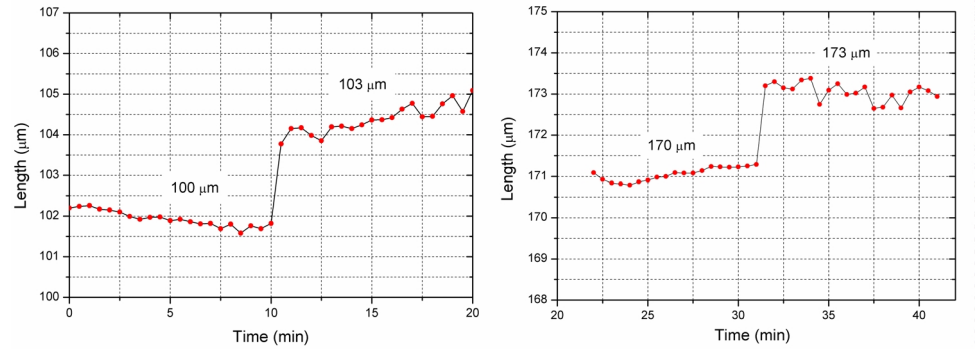

Fig. 4. Results of the time-stability and resolution experiment that consisted on monitoring a low-finesse Fabry-Perot cavity before and after a 3μm jump is applied to its length. The experiment was repeated for two initial lengths: a) 100μm and b) 103μm. Experiment carried out with an integration time of 5ms and 16 bits of A/D conversion.

Outside the range of lengths shown in Fig. 3, the performance of the technique drops very fast. There are two reasons for that. If the length of the cavity is bigger than, more or less, 220μm then the sinusoidal spectrum varies too fast for the system to determine its period. On the other hand, if the length of the cavity is below 90μm, then the period of the spectrum is bigger than the spectral width of the light source. This problem can be reduced simply by using a broader light source.

Other important characteristics of any sensor system are its temporal stability and resolution. To test the performance of the proposed interrogation system in these topics the following experiment was carried out: the sensing LFFPC was configured to be 100μm long, and the system was let evolve during 10 minutes. At the end of this period the cavity length was changed up to 103μm, and another 10 minutes period time elapsed. Later on the cavity length was increased up to 170μm and the whole process was repeated all over again. The photodetector linear array was configured with the same parameters as in the linearity experiment. The results of that experiment can be seen in Fig. 4. Both graphs show that the

#5299 - $15.00 US Received 15 September 2004; revised 3 November 2004; accepted 4 November 2004

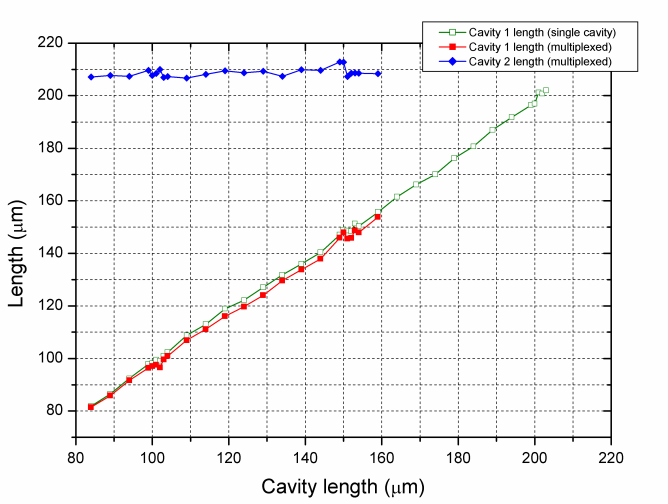

Fig. 5. Results of a length sweep applied to one of two multiplexed cavities (red squared line). The length recovered from the other cavity is also shown (blue dotted line). Besides, the result of the same sweep applied to a single non-multiplexed cavity is shown for comparison purposes (hollow green squared line). Experiment carried out with an integration time of 7ms and 16 bits of A/D conversion.

3μm-jumps applied to the cavity length are clearly visible. This implies that the resolution of the system is well below this threshold. In fact, taking into account that the maximum level of noise observed in the figure is around 0.5μm, this could be considered a good approximation to the unambiguous resolution of the system. On the other hand the temporal stability of the system, judging from the results presented in Fig. 4, doesn't seem to be very good. However, the drift observed in the figure (which is of 1μm at most in the different 10 minutes periods) is more due to the sensing LFFPC than to the system itself. Interferometers are known to be quite unstable devices which tend to drift a lot. This means that the temporal stability of the system is expected to be far better than the 0.1μm/min figure shown in the graphs.

Figure 5 shows the results of the interrogation of two multiplexed LFFPC when the integration time of the linear array was set to 7ms. One of them was set with a fixed cavity length of 209μm (blue dotted line) whereas the other one was swept from 85μm to 200μm (red squared line). Nevertheless, the graph of Fig. 5 only shows results up to 160μm. This is because from that point on the performance of the system drops considerably. The reason for this behavior is to be found in the demultiplexing algorithm. It has been previously said that it was based on a bandpass filtering of the recovered spectrum. This demands that the spectral contents of the chirped sinusoids corresponding to the multiplexed cavities were enough separated. Translating this to the cavity length domain, it imposes a restriction on the minimum value that the cavity lengths of the multiplexed LFFPC can differ. A good average value for that difference is 80μm. This restriction brings with it the reduction of the dynamic range since the perturbations applied to the cavities must be so that always ensure a minimum separation of more or less 80μm. Of course this figure is not fixed and depends on the cases, for example in the one shown in Fig. 5 the minimum separation that still provides a properly working situation is around 60μm.

Apart from the already mentioned reduction in the dynamic range, there is always some amount of crosstalk when multiplexing transducers. In this case the hollow-squared green line corresponding to the same cavity length sweep but applied to a non-multiplexed LFFPC is provided for comparison purposes. From that comparison it can be seen that the amount of crosstalk is very little in this case (less that 1% of the measured cavity length). Due to this fact, both the linearity and the accuracy of the system remain in acceptable levels.

#5299 - $15.00 US Received 15 September 2004; revised 3 November 2004; accepted 4 November 2004

4. Conclusion

The adaptation on an FBG interrogation technique for the demodulation of interferometric transducers has been presented in this paper. The concepts regarding the operating principle of this system have been reviewed. In particular a modified version of the MUSIC algorithm for the recovery of the path imbalance of interferometers from their spectra has been presented and discussed in detail. Finally, the experimental performance of the whole system has been experimentally tested. Thus, it has been shown that the resolution, linearity, accuracy and temporal stability have good values, even when multiplexed interferometric transducers are being simultaneously interrogated. Therefore, by means of the successful adaptation reported in this paper a new multi-transducer interrogation technique has been demonstrated.

Acknowledgment

This work has been co-supported by the Spanish CICYT TIC'2001-0877-C02-01 and the TIC-2001-4503-E projects.

#5299 - $15.00 US Received 15 September 2004; revised 3 November 2004; accepted 4 November 2004